A hybrid prediction tool for railway induced vibration

Pascal Bouvet[1], Brice Nélain[1], David Thompson[2], Evangelos Ntotsios[2], Andreas Nuber[3], Bernd Fröhling[3], Pieter Reumers[4], Fakhraddin Seyfaddini[4], Geertrui Herremans[4], Geert Lombaert[4], and Geert Degrande[4]

[1] Vibratec, 28 Chemin du petit bois, F-69131, Ecully, France
[2] University of Southampton, ISVR, Highfield, Southampton SO17 1BJ, UK
[3] Wölfel Engineering GmbH + Co. KG, Max-Planck Strasse 15, D-97204 Höchberg, Germany
[4] KU Leuven, Department of Civil Engineering, Kasteelpark Arenberg 40, B-3001 Leuven, Belgium
geert.degrande@kuleuven.be
https://silvarstar.eu

Abstract. One of the main objectives of the SILVARSTAR project is to develop a user-friendly frequency-based hybrid prediction tool to assess the environmental impact of railway induced vibration. This model will be integrated in the existing noise mapping software IMMI. Following modern vibration standards and guidelines, the vibration level in the building in each frequency band is expressed as the product of source, propagation and receiver terms. We explain the key quantities of interest (vibration velocity level, line source transfer mobility, force density, building correction factor), resulting in a framework that is ideally suited for a hybrid approach that combines experimental data with numerical predictions (e.g. pre-computed soil impedance and transfer functions), providing increased flexibility and applicability. We also discuss the validation of the prototype vibration prediction tool.

Keywords: railway induced vibration, hybrid vibration prediction model.

1 Introduction

Although rail is a sustainable and climate-friendly mode of transport, noise and vibration remain particular environmental concerns. People living near railways are becoming increasingly sensitive to high levels of noise and vibration, while the operation of sensitive equipment is hampered by high vibration levels. SILVARSTAR [1] is a two-year collaborative project under the Shift2Rail Joint Undertaking that aims to develop validated software tools and methodologies to assess the noise and vibration environmental impact of railway traffic. One of the objectives is to provide the railway community with a commonly accepted, practical and validated methodology and a user-friendly prediction tool for vibration. This tool will be used for environmental impact assessment of new or upgraded railways on a system level.

2 Methodology

2.1 General framework

The basic concept for the prediction of ground vibration in SILVARSTAR is to develop a frequency-based hybrid vibration prediction tool, following the general framework recommended in the ISO 14837-1:2005 standard [4]). This expresses the vibration level $A(f)$ in a building during a train passage as the product of a source term $S(f)$ for the vehicle-track interaction, a propagation term $P(f)$ for the soil and a receiver term $R(f)$ for the building:

$$A(f) = S(f)P(f)R(f) \tag{1}$$

or, equivalently, as a sum of terms in decibels. Equation (1) obtains the vibration level $A(f)$ by a product of three terms evaluated at the same frequency f, which omits the Doppler effect due to moving loads. However, it gives reasonable results if the train speed is relatively low compared with the wave velocities in the soil, while maintaining low calculation times [2]. Each of the terms in equation (1) can be represented by numerical predictions or by experimental data.

2.2 Fully empirical prediction scheme

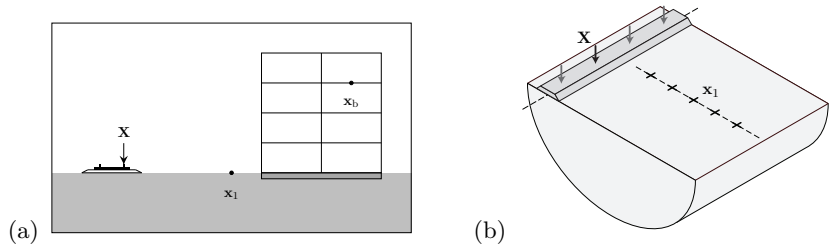

Fig. 1. (a) Source and receiver points for the FRA procedure and (b) excitation and receiver locations for line source transfer mobility measurements.

The empirical procedure for Detailed Vibration Assessment proposed by the Federal Railroad Administration (FRA) and the Federal Transit Administration (FTA) of the U.S. Department of Transportation [3, 9] conforms to the general framework recommended in ISO 14837-1:2005 and is used as a basis for the development of a hybrid vibration prediction tool. The vibration velocity level $\mathrm{L_v}(\mathbf{x}_\mathrm{b})$ at a receiver $\mathbf{x}_\mathrm{b}$ in the building (figure 1a) is defined as the root mean square value of the velocity during the stationary part of a train passage; it is expressed in decibels (dB ref 5×10^{-8} m/s) in one-third octave bands as a sum of source, propagation and receiver terms:

$$\mathrm{L_v}(\mathbf{x}_\mathrm{b}) = \mathrm{L_F}(\mathbf{X}, \mathbf{x}_1) + \mathrm{TM_L}(\mathbf{X}, \mathbf{x}_1) + \mathrm{C_b}(\mathbf{x}_1, \mathbf{x}_\mathrm{b}) \tag{2}$$

$\mathrm{L_F}(\mathbf{X}, \mathbf{x}_1)$ is the equivalent force density ($\mathrm{dB\,ref\,1N/\sqrt{m}}$) and a measure for the power per unit length radiated by the source. The vector $\mathbf{X}$ collects all source points on the rail heads (or other points on the track), while the receivers $\mathbf{x}_1$ are located on the ground surface.

The line source transfer mobility $\mathrm{TM_L}(\mathbf{X}, \mathbf{x}_1)$ ($\mathrm{dB\,ref}\, 5 \times 10^{-8} \frac{\mathrm{m/s}}{\mathrm{N/\sqrt{m}}}$) is a measure for the vibration energy transmitted through the soil relative to the power per unit length radiated by the source. It is derived from the superposition of point source transfer mobilities $\mathrm{TM_P}(\mathbf{X}_k, \mathbf{x}_1)$ for a series of n equidistant source points $\mathbf{X}_k$ with spacing h (figure 1b):

$$\mathrm{TM_L}(\mathbf{X}, \mathbf{x}_1) = 10 \log_{10} \left[h \sum_{k=1}^{n} 10^{\frac{\mathrm{TM_P}(\mathbf{X}_k, \mathbf{x}_1)}{10}} \right] \tag{3}$$

The force density $\mathrm{L_F}(\mathbf{X}, \mathbf{x}_1)$ is determined indirectly from the vibration velocity level $\mathrm{L_v}(\mathbf{x}_1)$ and the line source transfer mobility $\mathrm{TM_L}(\mathbf{X}, \mathbf{x}_1)$ by rearranging equation (2) (and omitting the building correction factor):

$$\mathrm{L_F}(\mathbf{X}, \mathbf{x}_1) = \mathrm{L_v}(\mathbf{x}_1) - \mathrm{TM_L}(\mathbf{X}, \mathbf{x}_1) \tag{4}$$

The receiver term or building correction factor $\mathrm{C_b}(\mathbf{x}_1, \mathbf{x}_\mathrm{b})$ can be quantified as a difference in vibration velocity level $\mathrm{L_v}(\mathbf{x}_\mathrm{b})$ at a point $\mathbf{x}_\mathrm{b}$ in the building, and $\mathrm{L_v}(\mathbf{x}_1)$ at a point $\mathbf{x}_1$ on the ground surface with the building present (figure 1a):

$$\mathrm{C_b}(\mathbf{x}_1, \mathbf{x}_\mathrm{b}) = \mathrm{L_v}(\mathbf{x}_\mathrm{b}) - \mathrm{L_v}(\mathbf{x}_1) \tag{5}$$

The vibration velocity levels can either be determined by measurements during a train passage, or they can be calculated with a train-track-soil-building model. They can also be computed as a combination of adjustment factors to account for soil-structure interaction at foundation level and attenuation and amplification within the building; in SILVARSTAR, a combination of adjustment factors from the RIVAS project [13] will be used.

The source can also be characterized by a vibration velocity level $\mathrm{L_v}(\mathbf{x}_\mathrm{ref})$ at a reference distance $\mathbf{x}_\mathrm{ref}$ (e.g. 8 m or 25 m [10]). When equation (2) is evaluated for $\mathrm{L_v}(\mathbf{x}_1)$ and $\mathrm{L_v}(\mathbf{x}_\mathrm{ref})$, the former can be expressed as:

$$\mathrm{L_v}(\mathbf{x}_1) = \mathrm{L_v}(\mathbf{x}_\mathrm{ref}) + \mathrm{L_F}(\mathbf{X}, \mathbf{x}_1) - \mathrm{L_F}(\mathbf{X}, \mathbf{x}_\mathrm{ref}) + \mathrm{TM_L}(\mathbf{X}, \mathbf{x}_1) - \mathrm{TM_L}(\mathbf{X}, \mathbf{x}_\mathrm{ref}) \tag{6}$$

If it is assumed that the force densities $\mathrm{L_F}(\mathbf{X}, \mathbf{x}_\mathrm{ref})$ and $\mathrm{L_F}(\mathbf{X}, \mathbf{x}_1)$ are equal, equation (6) is approximated as:

$$\mathrm{L_v}(\mathbf{x}_1) \simeq \mathrm{L_v}(\mathbf{x}_\mathrm{ref}) + \underline{\mathrm{TM_L}(\mathbf{X}, \mathbf{x}_1) - \mathrm{TM_L}(\mathbf{X}, \mathbf{x}_\mathrm{ref})} \tag{7}$$

The underlined term represents the difference in line source transfer mobilities at the receivers $\mathbf{x}_1$ and $\mathbf{x}_\mathrm{ref}$, for excitation at source locations $\mathbf{X}$.

2.3 Fully numerical prediction scheme using a modular approach

A semi-analytical train-track-soil interaction model (based on GroundVIB [6]) is integrated in the vibration prediction tool to compute the dynamic axle loads

and forces transmitted to the ground. The vehicle is represented by a multi-body model (e.g. a 10-DOF model, figure 2a). The ballasted or slab track (figure 2b) is modelled by Euler-Bernoulli beams for the rail (and slab) with resilient layers for rail pads, under-sleeper pads, ballast, and slab mat. Vehicle and track properties can be selected from a database or introduced as numerical values.

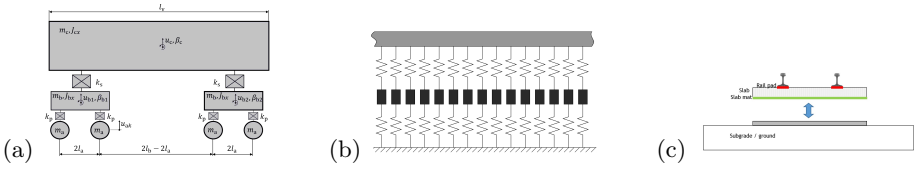

Fig. 2. (a) 10-DOF vehicle model, (b) ballasted track model, and (c) floating slab track on homogeneous soil.

The track is coupled to the soil over a finite width (figure 2c). The soil is represented by impedances in the frequency-wavenumber domain that are pre-computed for a range of track widths and soil properties (homogeneous and layered soils) using the MOTIV [7, 8] and TRAFFIC models [5]. The train-track-soil interaction problem is solved in the frequency domain, considering the excitation due to rail and wheel unevenness. The force transmitted to the subgrade is then estimated in the wavenumber-frequency domain and the free field ground response is calculated using pre-computed soil transfer functions. The response due to a train passage is obtained by summation of the contribution of each axle. The response of the building is estimated as in the empirical prediction scheme by means of building correction factors [13].

2.4 Hybrid prediction schemes

Hybrid prediction schemes, in which numerical and empirical data are combined following equation (2), are also included, providing more flexibity and applicability than purely experimental or numerical models.

In hybrid model 1, a numerical source model is combined with an empirical propagation term. The force density $\mathrm{L}_{\mathrm{F}}^{\mathrm{NUM}}(\mathbf{X})$ can be computed directly:

$$\mathrm{L}_{\mathrm{v}}^{\mathrm{HYB}}(\mathbf{x}_1) = \mathrm{L}_{\mathrm{F}}^{\mathrm{NUM}}(\mathbf{X}) + \mathrm{TM}_{\mathrm{L}}^{\mathrm{EXP}}(\mathbf{X}, \mathbf{x}_1) \tag{8}$$

Alternatively, the force density $\mathrm{L}_{\mathrm{F}}^{\mathrm{NUM}}(\mathbf{X}, \mathbf{x}_1)$ is computed indirectly as the difference between a predicted vibration velocity and line source transfer mobility:

$$\mathrm{L}_{\mathrm{v}}^{\mathrm{HYB}}(\mathbf{x}_1) = \mathrm{L}_{\mathrm{v}}^{\mathrm{NUM}}(\mathbf{x}_1) \underline{- \mathrm{TM}_{\mathrm{L}}^{\mathrm{NUM}}(\mathbf{X}, \mathbf{x}_1) + \mathrm{TM}_{\mathrm{L}}^{\mathrm{EXP}}(\mathbf{X}, \mathbf{x}_1)} \tag{9}$$

The underlined term can be interpreted as a correction term on the predicted vibration velocity level, accounting for the difference between the measured and predicted line source transfer mobility. Equations (8) and (9) are particularly useful to assess new rolling stock or a new railway line.

In hybrid model 2, a measured force density is combined with a predicted line source transfer mobility:

$$\mathrm{L_v^{HYB}}(\mathbf{x}_1) = \mathrm{L_F^{EXP}}(\mathbf{X}, \mathbf{x}_1) + \mathrm{TM_L^{NUM}}(\mathbf{X}, \mathbf{x}_1) \tag{10}$$

$$= \mathrm{L_v^{EXP}}(\mathbf{x}_1) \underline{- \mathrm{TM_L^{EXP}}(\mathbf{X}, \mathbf{x}_1) + \mathrm{TM_L^{NUM}}(\mathbf{X}, \mathbf{x}_1)} \tag{11}$$

which is useful to assess mitigation measures in the transmission path.

In all previous expressions, the building correction factor $\mathrm{C_b}(\mathbf{x}_1, \mathbf{x}_\mathrm{b})$ was omitted for brevity. When assessing vibration in a new building close to an existing railway, for example, the following hybrid approach can be employed:

$$\mathrm{L_v^{HYB}}(\mathbf{x}_\mathrm{b}) = \mathrm{L_F^{EXP}}(\mathbf{X}, \mathbf{x}_1) + \mathrm{TM_L^{EXP}}(\mathbf{X}, \mathbf{x}_1) + \mathrm{C_b^{NUM}}(\mathbf{x}_1, \mathbf{x}_\mathrm{b}) \tag{12}$$

while in case of an existing building next to a new-built railway, an empirical building correction factor $\mathrm{C_b^{EXP}}(\mathbf{x}_1, \mathbf{x}_\mathrm{b})$ can be added to equations (8) or (9).

2.5 Implementation of the vibration prediction model

The computational model is integrated into the existing noise mapping software IMMI, developed by Wölfel, and linked to a Geographical Information System (GIS), providing a software platform with Graphical User Interfaces (GUIs) that will allow engineers to perform noise and vibration environmental impact studies within the same integrated environment.

The use of pre-computed soil impedance and transfer functions for selected track widths and soil properties from a numerical database [12] considerably speeds up calculations and allows the user to assess in real-time the effect of changes in train, track, and soil parameters on axle loads and vibration.

An experimental database [12] of force densities, line source transfer mobilities, free field vibration and input parameters (rolling stock, track, unevenness, subgrade, soil,...) from well-documented measurement campaigns is integrated into the new hybrid vibration prediction tool.

The framework will also be oriented to compatibility with railway projects. The user will be able to import data from existing project databases dedicated to railway line development. Geographical and geotechnical data will be made importable through an interface with a GIS. The user will also be able to add data to the experimental database.

3 Validation of the prototype vibration prediction model

3.1 Modelling assumptions

A prototype vibration prediction model was developed based on the GroundVIB model, provided with a GUI. Three modelling simplifications are made in order to reduce computation times: (1) the computation of the track compliance in a stationary instead of a moving frame of reference; (2) the application of the dynamic axle loads at fixed positions (low-speed approximation neglecting the

Doppler effect); and (3) the assumption of incoherent instead of coherent axle loads. The influence of these modelling assumptions is assessed by means of a difference in vibration velocity level $\Delta \mathrm{L_v}(\mathbf{x}_1) = \mathrm{L_v^{approx}}(\mathbf{x}_1) - \mathrm{L_v^{ref}}(\mathbf{x}_1)$, where $\mathrm{L_v^{approx}}(\mathbf{x}_1)$ is the level predicted by the tool (accounting for the simplifications) and $\mathrm{L_v^{ref}}(\mathbf{x}_1)$ is a reference level computed with TRAFFIC. The assessment is made for a nominal InterCity (IC) train with 4 cars running at 50 km/h, 150 km/h, and 300 km/h on a ballasted track (unevenness FRA6) supported by soft ($C_\mathrm{s} = 100\,\mathrm{m/s}$), medium ($C_\mathrm{s} = 200\,\mathrm{m/s}$) and stiff ($C_\mathrm{s} = 400\,\mathrm{m/s}$) soil. Train, track, and soil parameters are detailed in [2, 11].

When computing the dynamic axle loads, the track compliance can, in very good approximation, be assessed in a stationary frame of reference. The vibration level difference $\Delta \mathrm{L_v}(\mathbf{x}_1)$ on the free field response for a train running at 300 km/h on a ballast track supported by soft soil is less than 1 dB when using the track compliance due to non-moving and moving loads [2, 11], and even smaller for lower train speeds and stiffer soils.

The low-speed approximation predicts the stationary part of the response by assuming fixed axle positions. Figure 3 illustrates that, at 16 m from the track, the vibration level difference $\Delta \mathrm{L_v}(\mathbf{x}_1)$ increases with increasing train speed and is larger than 10 dB in individual frequency bands at high speed. The differences mainly correspond, however, to a redistribution of energy into different bands, while the overall vibration level summed over all frequency bands is affected much less, with differences ranging from 2 to 3 dB [2].

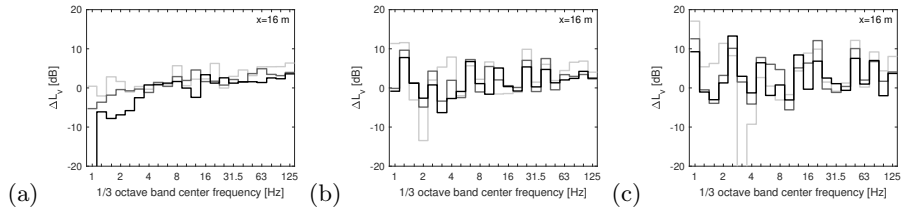

Fig. 3. Vibration velocity level difference $\Delta \mathrm{L_v}(\mathbf{x}_1)$ between the low-speed approximation and the moving train response at 16 m from the ballast track for the IC train running at (a) 50 km/h, (b) 150 km/h and (c) 300 km/h; soft, medium and stiff soil (light to dark lines).

Furthermore, the free field response is calculated assuming that the non-moving dynamic axle loads are incoherent, whereas in the full model the wheels are assumed to be excited by the same unevenness apart from a time lag. Figure 4a shows that, at 16 m from the track, largest differences at 50 km/h occur below 4 Hz; above 4 Hz, differences are less than 5 dB. At higher train speeds 150 km/h and 300 km/h (figures 4b-c), there is good agreement above 10 Hz and 20 Hz, respectively.

The Doppler effect has the largest influence, whereas the assumption of incoherent axle loads mainly affects the response at low frequencies. The effect on

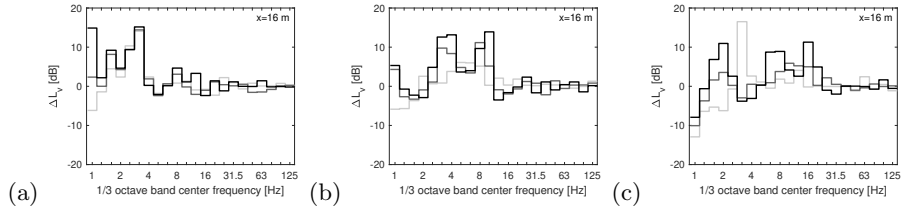

Fig. 4. Vibration velocity level difference $\Delta \mathrm{L_v}(\mathbf{x}_1)$ between the incoherent (non-moving)) load approximation and the coherent (non-moving) load reference case at 16 m from the ballast track for the IC train running at (a) 50 km/h, (b) 150 km/h and (c) 300 km/h; soft, medium and stiff soil (light to dark lines).

the track compliance is negligible. The combined effect of all three approximations at 16 m from the track is shown in figure 5 for the speed of 150 km/h; although there are significant differences in individual frequency bands, the spectrum shape is closely followed, while the overall vibration level summed over all frequency bands on average is 2-3 dB higher for the approximate model.

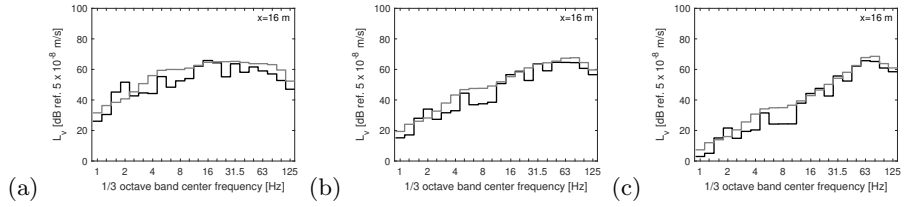

Fig. 5. Vibration velocity level $\mathrm{L_v}(\mathbf{x}_1)$ at 16 m from the ballast track for the IC train running at 150 km/h; (a) soft, (b) medium, and (c) stiff soil. Results of TRAFFIC for a moving train (black line) and the prediction tool with approximations (grey line).

3.2 Numerical validation

Results obtained with the prototype vibration prediction model are compared with those obtained with TRAFFIC for a ballast and slab track supported by homogeneous soil of varying stiffness; as before, track unevenness of class FRA6 is assumed, and an IC train with 4 carriages is running with a speed of 50 km/h, 150 km/h and 300 km/h. These case histories also form the basis for the numerical database [12], for which track width and soil properties are varied.

Identical modelling assumptions are made in both models; the only difference is that we use pre-computed soil impedance and transfer functions corresponding to a width of 3.0 m of the track-soil interface, while the actual width of 3.6 m is used in the reference model. Results are shown for the ballast track.

Figure 6 shows the line source transfer mobility $\mathrm{TM_L}(\mathbf{X}, \mathbf{x}_1)$ at 8 m, 16 m and 32 m from the ballast track on soft, medium and stiff soil. At low frequencies,

the line source transfer mobility is highest for the soft soil; the peak shifts to lower frequencies for increasing distance. At higher frequencies, the line source transfer mobility decreases due to material damping in the soil. For the medium and stiff soil, maximum response is observed at higher frequencies, while the effect of material damping is less pronounced. The results computed with the prediction tool and TRAFFIC are in excellent agreement up to 10 Hz. At higher frequencies, slightly higher values (1-3 dB) are obtained with the prediction tool due to the lower track width, with higher discrepancy at larger distance. Overall, the line source transfer mobility is in very good agreement, which demonstrates the correct modelling of the track-soil system in the prediction tool.

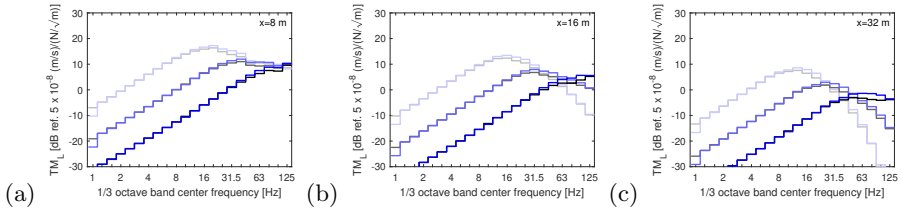

Fig. 6. Line source transfer mobility $\mathrm{TM_L}(\mathbf{X}, \mathbf{x}_1)$ at (a) 8 m, (b) 16 m, and (c) 32 m from the ballast track on soft, medium and stiff soil (light to dark lines). Results of TRAFFIC (grey lines) and the prediction tool (blue lines).

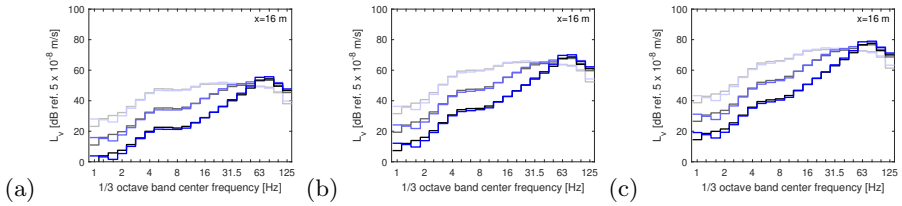

Fig. 7. Vibration velocity level $\mathrm{L_v}(\mathbf{x}_1)$ at 16 m from the ballast track on soft, medium and stiff soil (light to dark lines) for the IC train running at (a) 50 km/h, (b) 150 km/h and (c) 300 km/h. Results of TRAFFIC (grey lines) and the prediction tool (blue lines).

Figure 7 shows the vibration velocity level $\mathrm{L_v}(\mathbf{x}_1)$ at 16 m from the ballast track (on soft, medium and stiff soil) during the passage of the IC train at three speeds. For a speed of 50 km/h, the velocity level is highest for the soft soil up to 30 Hz. For the medium and stiff soil, a maximum value is reached at the P2 resonance close to 80 Hz. Around this frequency, the velocity level is lower for the soft soil due to the influence of material damping. At higher train speeds, the velocity level increases, but the trends are very similar to those found at 50 km/h. Between 30 Hz and 125 Hz the velocity level increases by approximately 16 dB when increasing the train speed from 50 km/h to 150 km/h, independent of the

soil stiffness. An additional increase of about 8 dB is observed by increasing the train speed to 300 km/h. Below 30 Hz, the velocity level predicted with TRAFFIC is 1-2 dB higher than with the prototype tool. At high frequencies, the prototype tool tends to predict a slightly higher velocity level.

Figure 8 shows the force density $L_F(\mathbf{X}, \mathbf{x}_1)$ based on the vibration velocity level and line source transfer mobility at 16 m from the track during the passage of the IC train at 50 km/h, 150 km/h and 300 km/h. Since the influence of the soil stiffness on the dynamic axle loads is limited below 50 Hz, the force density is almost identical for the three soil types up to this frequency. At high frequencies, the force density is higher for the soft soil. The force density increases with increasing train speed, as the velocity level (figure 7). The force densities computed with the prediction tool and TRAFFIC are in very good agreement. The discrepancy is limited to 3 dB in each frequency band and is due to the different track width when pre-computing the soil impedance and transfer functions.

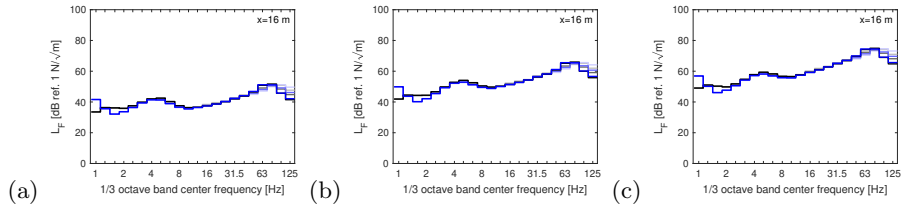

Fig. 8. Force density $L_F(\mathbf{X}, \mathbf{x}_1)$ at 16 m from the ballast track on soft, medium and stiff soil (light to dark lines) for the IC train running at (a) 50 km/h, (b) 150 km/h and (c) 300 km/h. Results of TRAFFIC (grey lines) and the prediction tool (blue lines).

3.3 Experimental validation

The experimental case history of Lincent (Belgium) was identified as a benchmark to be included in the hybrid prediction model. Transfer functions between the track and the free field and vibration during train passages (InterCity, ICE, and Thalys) were processed (in terms of vibration levels and line source transfer mobilities) to ensure compatibility with the hybrid vibration prediction model. Overall good correspondance between measured and predicted results is reported [2].

4 Conclusion

The proposed modular approach provides full modelling flexibility at each stage of the design process. Embedding it in existing software simplifies the modelling process, as fewer interfaces are needed. Extensive validation and approval testing increases confidence levels. The prediction tool will enable the assessment of vibration levels for both large-scale studies and more detailed investigations for new and upgraded railway lines.

References

1. G. Degrande, G. Lombaert, E. Ntotsios, D.J. Thompson, B. Nélain, P. Bouvet, S. Grabau, J. Blaul, and A. Nuber. State-of-the-art and concept of the vibration prediction tool. SILVARSTAR project GA 101015442, Deliverable D1.1, Report to the EC, May 2021.
2. G. Degrande, G. Lombaert, F. Seyfaddini, G. Herremans, P. Reumers, E. Ntotsios, D.J. Thompson, B. Nélain, P. Bouvet, B. Fröhling, and A. Nuber. Validation of the prototype vibration prediction tool against documented cases. SILVARSTAR project GA 101015442, Deliverable D1.3, Report to the EC, June 2022.
3. C.E. Hanson, J.C. Ross, and D.A. Towers. High-Speed Ground Transportation Noise and Vibration Impact Assessment. Technical Report DOT/FRA/ORD-12/15, U.S. Department of Transportation, Federal Railroad Administration, Office of Railroad Policy and Development, September 2012.
4. International Organization for Standardization. *ISO 14837-1:2005 Mechanical vibration - Ground-borne noise and vibration arising from rail systems - Part 1: General guidance*, 2005.
5. G. Lombaert, S. François, and G. Degrande. TRAFFIC Matlab toolbox for traffic induced vibrations. Report BWM-2012-10, Department of Civil Engineering, KU Leuven, November 2012. User's Guide Traffic 5.2.
6. B. Nélain, N. Vincent, and E. Reynaud. Towards hybrid models for the prediction of railway induced vibration: numerical verification of two methodologies. In G. Degrande and G. Lombaert, editors, *Proceedings of the 13th International Workshop on Railway Noise, IWRN13*, pages 1–8, Ghent, Belgium, September 2019.
7. E. Ntotsios, D.J. Thompson, and M.F.M. Hussein. The effect of track load correlation on ground-borne vibration from railways. *Journal of Sound and Vibration*, 402:142–163, 2017.
8. E. Ntotsios, D.J. Thompson, and M.F.M. Hussein. A comparison of ground vibration due to ballasted and slab tracks. *Transportation Geotechnics*, 21(100256), 2019.
9. A. Quagliata, M. Ahearn, E. Boeker, C. Roof, L. Meister, and H. Singleton. Transit Noise and Vibration Impact Assessment Manual. FTA 0123, U.S. Department of Transportation, Federal Transit Administration, John A. Volpe National Transportation Systems Center, September 2018.
10. D. Stiebel, H. Brick, R. Garburg, G. Schleinzer, H. Zandberg, B. Faure, A. Pfeil, S. Thomas, A. Guiral, and M. Oregui. Specification of model requirements including descriptors for vibration evaluation. FINE2 project GA-881791, Deliverable D8.1, Report to the EC, 2020.
11. D. Thompson, E. Ntotsios, P. Bouvet, B. Nélain, S. Barcet, A. Nuber, B. Fröhling, P. Reumers, F. Seyfaddini, G. Herremans, G. Lombaert, and G. Degrande. The influence of model assumptions in a hybrid prediction tool for railway induced vibration. In *Proceedings of the 51st International Congress and Exposition on Noise Control Engineering, Inter-Noise 2022*, Glasgow, United Kingdom, August 2022.
12. D.J. Thompson, E. Ntotsios, G. Degrande, G. Lombaert, G. Herremans, T. Alexiou, B. Nélain, S. Barcet, P. Bouvet, B. Fröhling, and A. Nuber. Database for vibration emission, ground transmission and building transfer functions. SILVARSTAR project GA 101015442, Deliverable D2.1, Report to the EC, January 2022.
13. M. Villot, C. Guigou, P. Jean, and N. Picard. Procedures to predict exposure in buildings and estimate annoyance. RIVAS project SCP0-GA-2010-265754, Deliverable D1.6, Report to the EC, 2012.